UJEAS

UNIZIK JOURNAL OF ENGINEERING AND APPLIED SCIENCES

UNIZIK Journal of Engineering and Applied Sciences 3(4), September (2024), 1208 - 1219
Journal homepage: https://journals.unizik.edu.ng/index.php/ujeas
PRINT ISSN: 2992-4383 || ONLINE ISSN: 2992-4391

Empirical Analysis of Energy Absorption by Fractured Carbon Fibre Reinforced Polymer based on Materials Loading Rate and Crush Distance.

C. I. Nwoye, C. C. Emekwisia*, C. N. Nwambu, C. U. Uzochukwu, and K. C. Nnakwo
Chemical Systems and Data Research Laboratory, Department of Metallurgical and Materials Engineering, Nnamdi Azikiwe University, Awka, Nigeria.

*Corresponding Author's E-mail: cc.emekwisia@unizik.edu.ng

Abstract
This paper presents a successful attempt to empirically analyze the energy absorption E, by fractured carbon fibre reinforced polymer based on the materials loading rate ϴ, and crush distance δ. This followed derivation of a model expression relating the energy absorbed, loading rate and crush distance. The carbon fibre reinforced polymer was prepared, following a well detailed step-wise route, involving monomer polymerization, spinning of resulting precursor to form fibre, oxidation/carbonization of fibre to form carbon fibre and then coating to embellish the material. At decreasing peak crush force, the energy absorption decreases while loading rate and crush distance increases and decreases respectively. In the course of the model derivation, the range of crushing distance and loading rate considered are 0.04162 – 0.05848m and 0.001 - 10.0 m/s respectively. The validity of the derived model expressed as; E = ȟeκδ - ϐlnϴ + N was rooted in the core expression E+ ϐlnϴ ≈ ȟeκδ+ N where both side of the expression correspondingly near-equal. Results generated from both experiment and model prediction indicates that energy absorbed decreases with increased loading rate and decreased crush distance. Evaluated results show that the correlations between the energy absorbed and loading rate & crush distance are 0.9780 and 0.9358 & 0.9795 and 0.9810, using model-predicted and experimental results respectively. For every change in the loading rate and crush distance, the overall standard error incurred on predicting the energy absorbed by the fractured composite, relative to experimental results is < 0.05%. The maximum differential between the experimentally determined and model-predicted energy absorption by fractured carbon fibre reinforced polymer is – 0.1046kJ. The energy absorbed by the fractured composite per unit loading rate and crush distance are -1.875×10^{-2} & $-2.26 \times 10^{-2} \mathrm{KJsm^{-1}}$ and 19.5567 and $23.5724\ \mathrm{KJsm^{-1}}$ as evaluated from experimental and derived model results.

Keywords: Energy Absorption, Carbon Fibre Reinforced Polymer, Loading Rate, Crush Distance.

1. Introduction

Composite materials, or just composites, as they are often referred to, consist of two or more distinct constituents or phases made from engineered or naturally-occurring materials, where each material has significantly different physical or chemical properties, which remain separate and distinct within the finished/combined structure. (Emekwisia 2020). Researchers (Lau, et. al., 1995; Shanmugam, et. al., 2002; Hernandez-Castaned, Sezer, and Li 2011; Santhanakrishnan, Krishnamurthy, Malhotra 1988) have shown that composites will eventually become the most wanted materials type in industry and are already gaining wide acceptance in, for example, construction, furniture, packing, flooring, panelling and automotive. In addition, composites are applied in many high-tech industries, such as aerospace and defence (Shanmugam, et. al., 2002).

Fiber-reinforced polymer-matrix (FRP) composites with typical fiber volume fractions of 50 - 60% are increasingly used in high-performance aircraft and spacecraft structures, mainly based on their comparatively high specific strength and stiffness which derive from their relatively low density. This trend is expected to continue due to the increasing demand for energy-saving propulsion systems for aircraft and spacecraft for which weight reductions are a key element. An important issue for these applications is impact resistance and durability under the rather severe service conditions in the aerospace environment. FRP composites are prone to damage from initiation and propagation of delaminations in the matrix layer between the fibers or from fiber-matrix de-bonding. Fracture mechanics of FRP composites has to consider the anisotropic morphology of the material, which affects the location of the delaminations (Williams 1989). Delaminations located in the matrix between the planes defined by the fiber layup or the fiber plies are hence, called inter-laminar. Initiation of such delaminations or of fiber-matrix de-bonding is caused by the impact of “foreign” objects (e.g., bird strike, dropping of tools, collision with other vehicles), followed by propagation and growth due to cyclic thermo-mechanical service loads, if the applied stresses are large enough. Delaminations can also initiate from processing induced defects in FRP composite parts, such as machining, cutting or drilling (Lasri, Nouari and Mansori 2011; Shetty et. al., 2017). Residual stresses from processing and manufacturing (e.g., near voids), or at material discontinuities and geometric features, e.g., edges, holes and ply drop-offs, also provide initiation sites for delaminations or contribute to their propagation and growth. This has spurred research into improving delamination resistance or fracture toughness of FRP laminates.

Fracture mechanics is the scientific discipline dealing with the behavior of cracks in materials under applied loads, stresses, or deformations. Fracture mechanics tests for quantifying delamination resistance determine the change in strain energy per unit area of delamination, i.e., the strain energy release rate which is denoted by the symbol G. Assessing the long-term performance of FRP composites for aerospace applications, notably of their delamination resistance, also requires consideration of the effects of the respective service load spectra and of the related environmental exposure. Most FRP composites have a comparatively high specific stiffness and show essentially linear-elastic behavior under mechanical loads. Therefore, delamination propagation in FRP composites can be analyzed with the methods of Linear Elastic Fracture Mechanics (LEFM). This avoids the complexity of dealing with elastic plastic or plastic fracture mechanics in this class of materials in most cases (Williams 2011). Test methods are further divided into quasi-static (typical load rates of a few mm/ min), intermediate and high rates (around 1 m/s and several m per second, respectively) and cyclic load tests (with a choice of tension-tension, tension-compression or compression-compression loads) at constant or variable frequency and constant or variable load or displacement amplitude. The R-ratio describes the ratio between minimum and maximum stress (essentially load). The symbol R is also used for displacement ratio if the test is performed under displacement control rather than load control. The scope of standardized fracture mechanics test methods usually specifies inter-laminar delamination resistance or fracture toughness of FRP composites with carbon- or glass-fiber reinforcements (CFRP and GFRP, respectively), which are the typical materials used in round robin testing for the development of the standard test procedures. Besides inter laminar delamination propagation (i.e., extension of the delamination in the polymer matrix between fiber layers, or fiber plies), delamination can also propagate in the intra-laminar direction (i.e., between fibers, but normal to the orientation of the fiber plies), or even in trans-laminar direction (i.e., normal to the fiber ply orientation, resulting in fiber or fiber ply breaking).

FRP composites in some applications use hybrid fiber reinforcements (e.g., a mixture of carbon and glass fibers, or one of these with fibers made from another material). “Fibers” as reinforcement can be “continuous” or “short” and are embedded in a polymer matrix. Continuous fibers can be fully or mainly aligned in one single direction (if “fully” aligned, the laminates are called unidirectional), in different planar directions (this is called multi-directional), or even in three spatial dimensions (e.g., emulating “textile”-type reinforcements). “Short” fibers have lengths in the range between a few centimeters and fractions of 1 mm down to about 0.1 mm.

In spite of extensive developments over the last 30 years, not all possible combinations of loading modes, load-rate as well as polymer types and fiber layups have yielded standards yet. Some scientists [Gillespie 1991; Tay 2003; Davies 2008; Brunner 2008; Brunner 2018) have reviewed the status of delamination resistance test developments. Furthermore, selected challenges in the field of fracture and fatigue fracture of FRP composites have recently shown (Brunner 2018) that cyclic fatigue fracture loading can be performed under tension, tension-compression, or compression-compression. Some cyclic fatigue loading modes have been explored in fracture mechanics research. Mode III cyclic fatigue has been explored (Donaldson and Mall 1989), but the split cantilever beam specimen yield varying mode II and mode III contributions even in quasi-static tests (Martin 1991). Tests on GFRP woven epoxy were performed at low temperatures under mode III cyclic fatigue loading (Miura et al. 2009), mixed mode I/II loading (Shindo et. al. 2011), and mixed-mode I/III (Miura et. al. 2014). On the other hand, mixed-mode I/II fatigue fracture testing of FRP composites were investigated (Jaeck et. al. 2018; Rubiera et. al. 2018) at room temperature.

The Finite Element model (FE) (Johnson, Pickett, and Rozycki 2001; Greve and Pickett 2006) involves stacked shell elements for the composite laminate connected through cohesive interfaces to model delamination failure. This can be described as a 2.5D FE model, where the stacked shell technique allows a composite laminate to split into plies or sub-laminates when the cohesive interface fails, and delamination occurs. The ply damage and failure model (Ladeveze and Le Dantec 1992) is associated with damage evolution equations that have a specific form requiring additional parameters to be determined from specimen tests. The ply properties assigned were based on a composite ply damage model for unidirectional (UD) composites with shear plasticity (Ladeveze and Le Dantec 1992), which was extended to fabric plies (Johnson, Pickett, and Rozycki 2001). The plasticity model (Johnson et. al. 2015) is about the shear plasticity with an elastic domain function and hardening law, which requires additional cyclic shear tests for the plies to determine a power-law plastic hardening function. Series of models (Johnson, Pickett, and Rozycki 2001; Greve and Pickett 2006; Ladeveze and Le Dantec 1992; Johnson et. al. 2015) which evaluate fracture (in carbon-fibre made aircraft components), and corresponding energy absorption are specifically based on composites quasi-static test properties, although polymer composites exhibit rate-dependent behavior under dynamic crash loads. However, no existing mathematical expression or model has calculated the energy absorption associating fracture (on the aircraft structures) based on the crush distance and loading rate on the materials. This prompted the need for the present work to fill in the gap. The present work aims at develop an empirical model which will predict the energy absorption associating fracture of carbon fibre reinforced polymer (designated for aircraft structures), based on loading rate on the material and crush distance. It is expected that the model if derived, shall predict the energy absorbed, (following fracture of the composite) within the experimental result range, providing the input parameters are within the boundary condition

2.0 Material and methods

2.1 Manufacturing processes for carbon fibre composite for aerospace applications.

2.1.1 Prepreg/autoclave processes.

2.1.1.1 Sub-sub-subheading fourth level heading.

Manufacturing of carbon fibre composite structures involves use of prepreg tape to produce the structural components. Fibers are initially combined into unidirectional tows (bundles) of fibers combined into fabrics, e.g., by weaving or knitting. The vast majority of the tows employed in woven, braided or knitted reinforcements comprise low twist or untwisted continuous filament yarns. Three-dimensional technical textiles can be produced by weaving (Bisagni et. al. 2005), knitting (Federal Aviation Administration. AC20-107B), and braiding (Hachenberg 2002), or as non-crimp fabrics. Sheets of fibers are soaked or coated in the partially cured resin. Controlled pre-impregnation using dip coating and lick roll technology is used to apply a uniform amount of uncured resin to the reinforcement. The resin contains both the base matrix resin and hardeners. The sheets are protected on both sides by the backing paper or film to stop them from sticking. (EERE 2017)

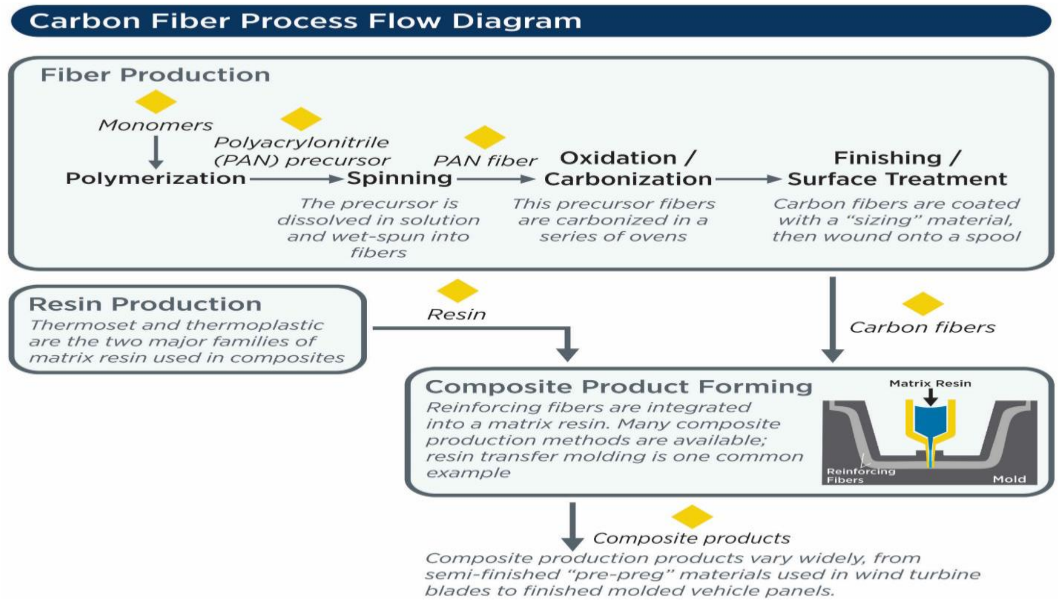

Figure 1: Process flow diagram for carbon fiber reinforced polymer composite manufacturing Source: (EERE 2017). [29]

They must be stored at low temperatures to avoid the further curing and cross-linking of the resin matrix, which occurs at room temperature. Rolls of prepreg are stored under refrigerated conditions for a given period of time before the shelf life of the product expires. A sophisticated materials handling system is required to track all the materials to ensure that out-of-life prepreg is not used. Prior to processing, rolls are removed and allowed to thaw and condition. After reaching room temperature, the fabric is cut into shaped plies, taking into account fiber orientation. Computer-based nesting is used to optimize fabric utilization. These plies are labeled to ensure they are used in the correct sequence. Plies of prepreg are cut into the appropriate shape either by hand or by an automated process, such as a Gerber cutter system. Plies are placed in a precise order and orientation on the surface of a tool made in the shape of the component to be manufactured. Since the layup sequence and orientation of the plies is critical to the performance of the composite, the plies are hand laid into the thoroughly degreased and clean molding tool correctly. Constant inspection and signing-off of the layup at each stage is necessary to ensure performance and quality. Where the component comprises a large number of plies, frequent debaulking is required; i.e., the layup is compressed under vacuum, after which a further series of plies are laid-in. Once the layup is completed, a layer of release film is laid on top of the ply layup to prevent the resinous stack of plies from adhering to the fibrous breather cloth which is used to absorb any excess resin and distribute the applied pressure evenly over the layup. Since a single tool surface is utilized, a good finish is secured on only one surface of the component, the other surface being in contact with the release film(Johnson et. al. 2015).

Table 1: Variation of absorbed energy by carbon fibre reinforced polymer with its loading rate, peak crush force and crush distance (Johnson et. al. 2015).

(E)	(ϴ)	(F)	(δ)
1.420	0.001	31.86	0.05848
1.156	1.0	31.44	0.05389
0.891	2.0	31.01	0.04929
0.880	2.5	30.49	0.04869
0.825	5.0	27.88	0.04567
0.783	7.5	31.79	0.04365
0.741	10.0	35.69	0.04162

Computational analysis of the experimental results shown in Table 1, resulted to Table 2 which indicate that;

$$E + ß \ln \theta \approx Ƅe^{\kappa\delta} + N \quad (1)$$

$$E = Ƅe^{\kappa\delta} - ß \ln \theta + N \quad (2)$$

The derived model shown as a mathematical expression in (2) predicts the total energy absorbed by fractured carbon fibre reinforced polymer subjected to crush force, based on material loading rate and crush distance. The variables E, ϴ and δ are total energy absorbed by fractured carbon fibre reinforced polymer (kJ), material loading rate (m/s) and crush distance (m) respectively. The table also show the peak crush force F (KN). The derived model is referred to as Nwoye`s Model for evaluating the total energy absorbed by carbon fibre reinforced polymer during fracture or Nwoye`s TEC-FIREP Model. The absorbed energy is basically the work done by the crush force. It is the area under the crush force – displacement curve. The equalizing constants; Ƅ, к, ß and N are 0.07, 38.91, 0.0359 and 0.4815 respectively. The constants which are conversion factor were generated using a software (Nwoye 2008). The interaction between these constants and variables ensures that the numerical value and units at both sides of the derived model are approximately equal and dimensional same respectively.

$$E_{absorbed} = \sum_{1=2}^{N=1} P_i \left(\frac{\delta_{i+1} - \delta_{i-2}}{2}\right) \quad (3)$$

The mathematical expression (Cheng 2005) in (3) is an experimentally determined conventional formular which calculates the total energy absorbed by fractured composite. The energy is calculated as the product of the crush force P(N) and half the crush distance (m).

Substitution of (3) into (2), gives;

$$E_{absorbed} = \sum_{1=2}^{N=1} P_i \left(\frac{\delta_{i+1} - \delta_{i-2}}{2}\right) = Ƅe^{\kappa\delta} - ß \ln \theta + N \quad (4)$$

The expressions (4) shows that $E_{absorbed}$ = E, providing the numerical differential between both expressions is zero or negligible. It therefore implies that any of the parameters in (4) can be evaluated at known values of the others.

3.0 Results and Discussions
3.1 Boundary and Initial Conditions

Carbon (filler), interacted with the matrix (polyester resin). The fracture on the composite is induced by the crush force, which in turn is affected by the crush distance and loading rate. During the model derivation, the considered range of energy absorbed, crush distance and loading rate on the material are 0.741 – 1.42 kJ, 0.04162- 0.05848 m and 0.001 – 10 m/s respectively.

Table 2: Variation of E+ ßlnϴ with Ƅeκδ+ N

E + ßlnϴ	Ƅeκδ+ N
1.1720	1.1628
1.1560	1.0514
0.9159	0.9580
0.9129	0.9469
0.8828	0.8953
0.8553	0.8641
0.8237	0.8350

Table 1 shows the variation of energy absorbed by fractured carbon fibre reinforced polymer with the material loading rate and crush distance. The core model structure expressed in (1) is the pivot on which the validity of the model is rooted. This is based on the fact that both sides of the structure are correspondingly almost equal. Table 2, derived from experimental results in Table 1 gives a numerical confirmation of the model structure, considering the closeness of the evaluated structure components.

3.2 Model Validity

The derived model was also validated by comparing the predicted results with the experimental, through graphical, statistical and deviational analysis.

3.2.1 Graphical Analysis

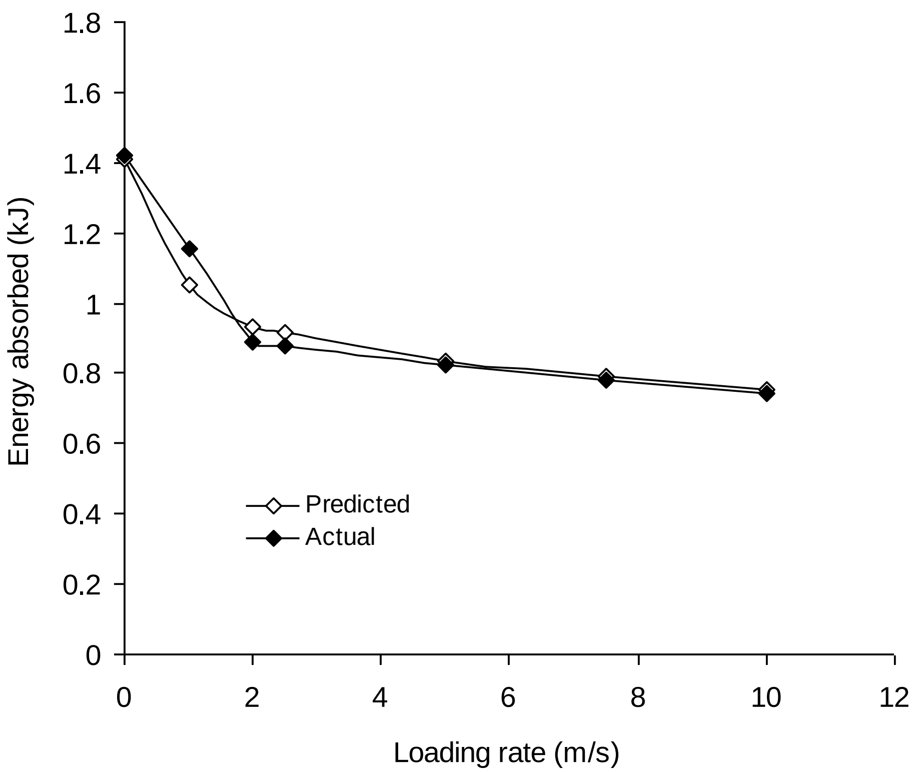

Figure 2: Comparison of energies absorbed by carbon fibre reinforced polymer (relative to loading rate) as evaluated from actual results and derived model.

Curves of experimental and model-predicted results, represented by absorbed energies, relative to loading rate and crush distance are shown in Figure 2 and Figure 3 respectively. These figures are characterized by similar trend and spread of results points` distribution. The absorbed energies plotted in these figures show inverse and direct relationships with loading rate and crush distance, and so emphasize negative and positive slopes respectively.

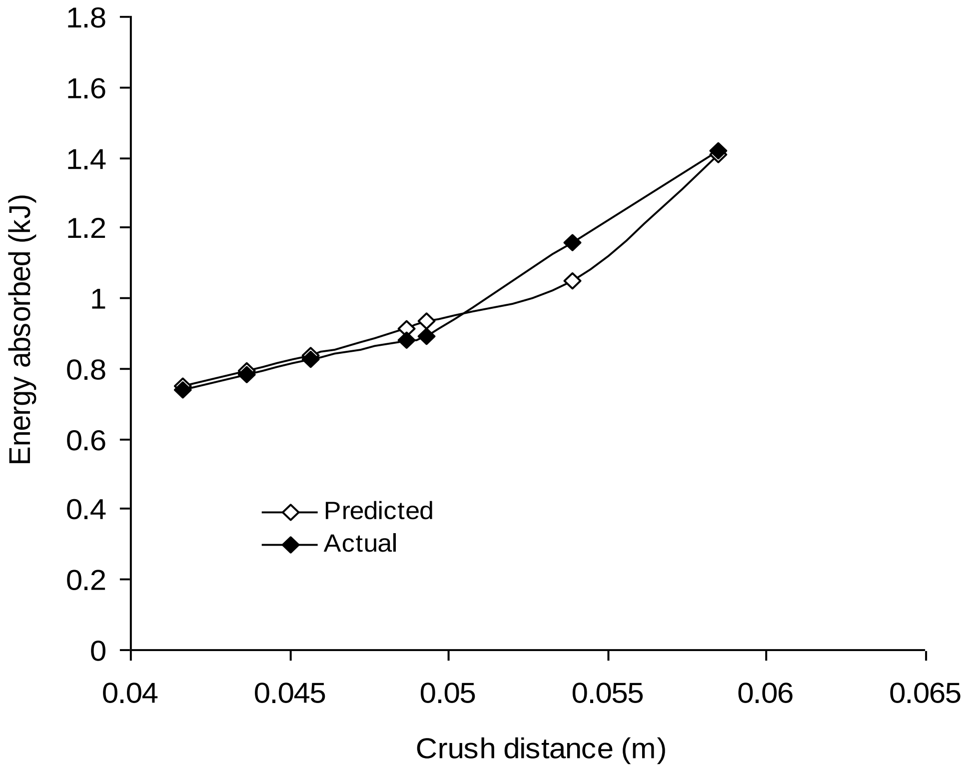

Figure 3: Comparison of energies absorbed by carbon fibre reinforced polymer(relative to crush distance) as evaluated from actual results and derived model.

3.2.2 Statistical Analysis

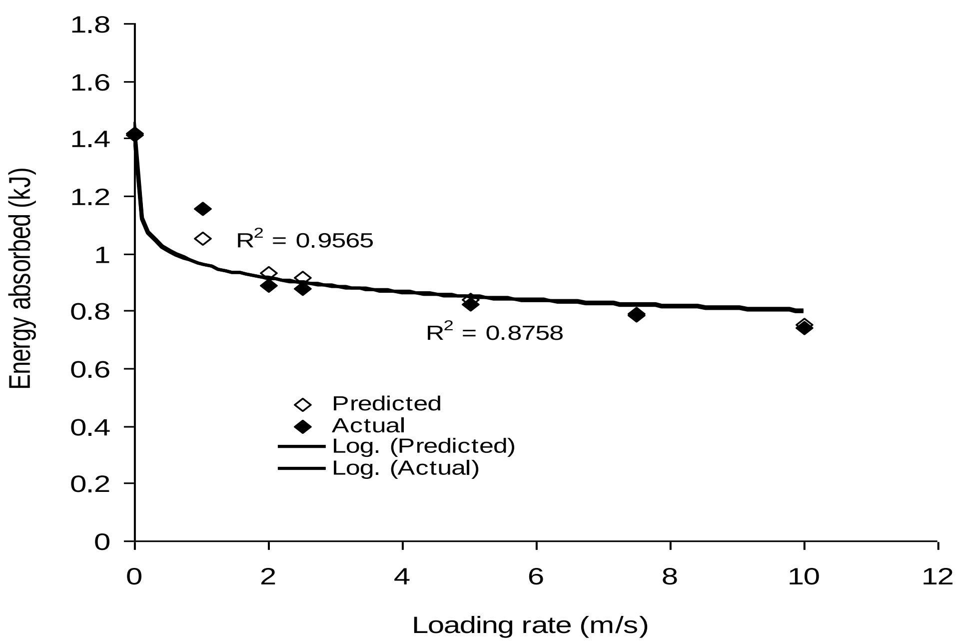

Figure 4: Coefficient of determination between energy absorbed by carbon fibre reinforced polymer and loading rate as evaluated from actual results and derived model.

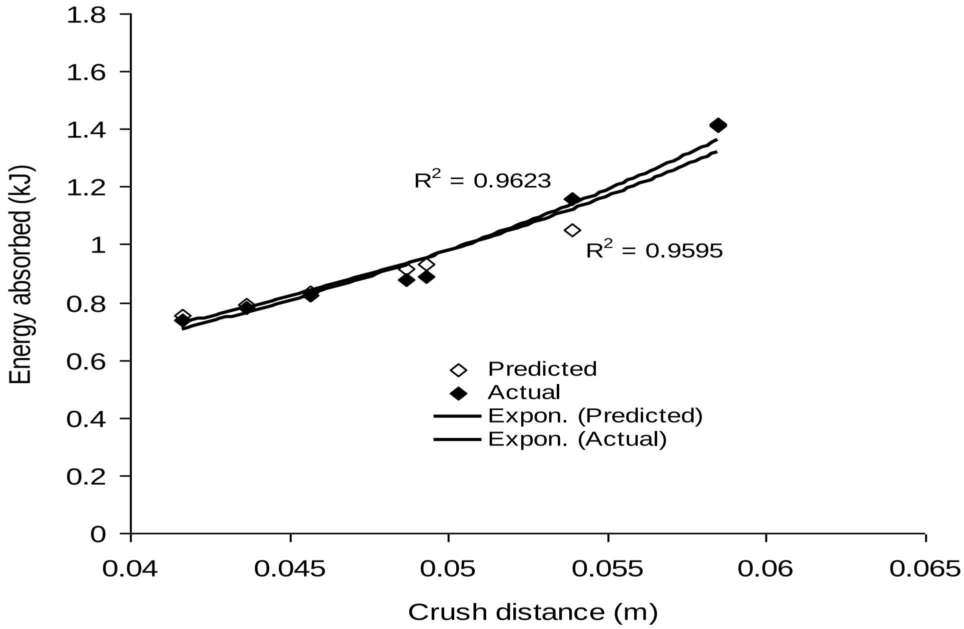

Figure 5: Coefficient of determination between energy absorbed by carbon-fibre reinforced polymer and crush distance as evaluated from actual results and derived model.

Correlations evaluated from the coefficients of determination R2 shown in Figure 4 and Figure 5, between energy absorbed and loading rate & crush distance are 0.9780 and 0.9358 & 0.9795 and 0.9810, using model-predicted and experimental results respectively. Comparative analyses of these correlations indicate a better line fitness with crush distance.

For every change in the loading rate and crush distance, analysis of the overall standard error incurred on predicting the energy absorbed by the fractured polymeric material, relative to experimental results revealed a value < 0.05%. This gives a model confidence level above 99%. The significance of the evaluated correlations and standard error is an indication of the model`s functionality and validity.

Table 2: Differential between experimentally determined and model-predicted energy absorption of carbon fibre reinforced polymer.

$\mathbf{E}$	$\Delta\mathbf{E} = \mathbf{E}_{M} - \mathbf{E}_{\varepsilon}$
1.420	-0.0092
1.156	-0.1046
0.891	0.0421
0.880	0.0340
0.825	0.0125
0.783	0.0088
0.741	0.0113

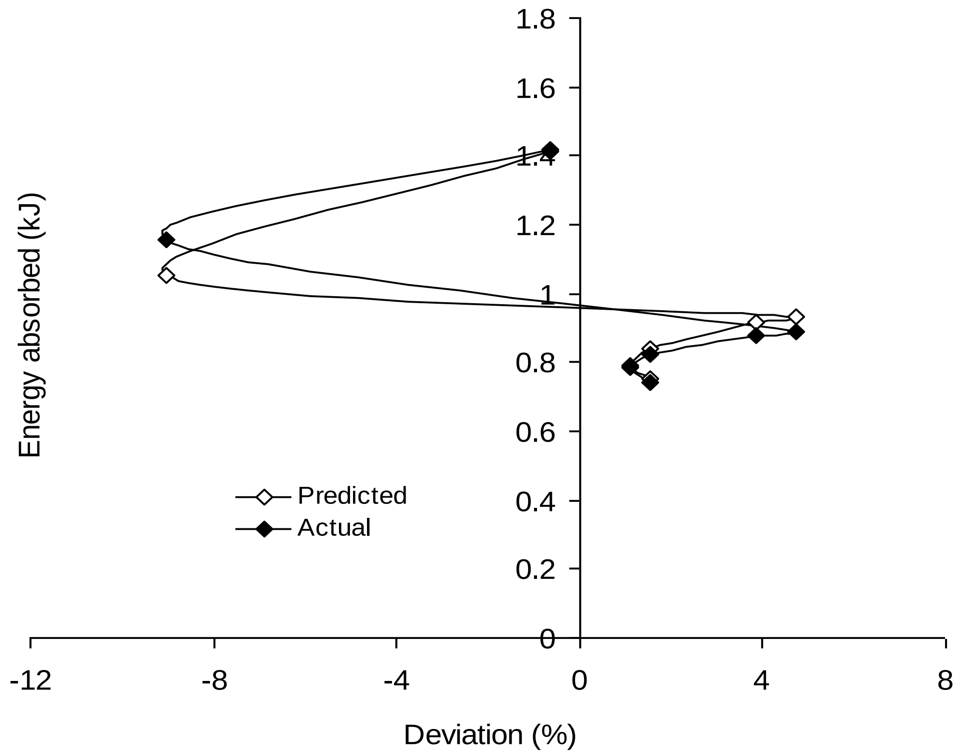

Figure 6: Variation of model-predicted energy absorption (of carbon-fibre reinforced polymer) with its corresponding deviation from experimental results.

Table 3 outlines negligible differentials between experimentally determined and corresponding model-predicted energy absorbed. This gives a significant level the derived model`s functional and admissible. Based on the foregoing, it is instructive to state that expressions (2) and (3) can be equated to each other as in (4) to evaluate the known. The table also shows that these differentials have positive and negative values, relative to the corresponding experimental results. This indicates increased and decreased model-predicted values respectively.

The deviation of model-predicted E from corresponding experimental results is shown in Figure 6. The figure indicates that the overall maximum deviation of model-predicted E is 9.05%. This gives operational model confidence levels above 90%. It is also shown that the least and highest magnitude of deviations of the model-predicted E are – 0.65 and -9.05% respectively. Invariably these deviations correspond to the energies absorbed: 1.4108 & 1.0514 kJ, loading rates: 0.001 & 1.0 m/s and crush distances: 0.05848 & 0.05389m respectively. Following series of highlighted evaluations, the overall model confidence level places between 90 and 97%.

$$\mathrm{E}\theta = \frac{\mathrm{E}}{\theta} \quad (5)$$

Re-written as

$$\mathrm{E}\theta = \frac{\Delta\mathrm{E}}{\Delta\theta} \quad (6)$$

The expression (6), is detailed as

$$E\Theta = \frac{E_2 - E_1}{\Theta_2 - \Theta_1} \qquad (7)$$

Where

ΔE = Change in the energies absorbed E_2, E_1 at two polymer loading rates Θ_2 Θ_1.

Plotting points (2, 0.891) & (10, 0.741) and (2, 0.9331) & (10, 0.7523) as shown in Figure 2, designated as (Θ_1, E_1) and (Θ_2, E_2) for experimental and model-predicted results, substituting them into the expression (7), gives the slopes: -1.875 x 10^{-2} and -2.26 x $10^{-2}KJsm^{-1}$, as their respective energy absorbed per unit loading rate.

Energy absorbed by fractured polymer per unit crush distance $E_\delta KJsm^{-1}$ was calculated from the expression;

$$E_\delta = \frac{E}{\delta} \qquad (8)$$

Re-written as

$$E_\delta = \frac{\Delta E}{\Delta \delta} \qquad (9)$$

The expression (9), is detailed as

$$E_\delta = \frac{E_2 - E_1}{\delta_2 - \delta_1} \qquad (10)$$

Where

$\Delta\delta$ = Change in the crush distances δ_2, δ_1

Points (0.04929, 0.891) & (0.04162, 0.741) and (0.04929, 0.9331) & (0.04162, 0.7523) were plotted as shown in Figure 3. On designating these points as (δ_1, E_1) and (δ_2, E_2) for experimental and model-predicted results, and substituting them into the expression (10), gives 19.5567 and 23.5724$KJsm^{-1}$ as the slopes. This translates into energy absorbed per unit crush distance.

The slopes evaluated based on the loading rate show negative signs. This basically indicates that the associated curves are oriented in the negative plane. The real values are therefore the modulus of the evaluated parameter.

4.0. Conclusion

Empirical analysis of energy absorption E by fractured carbon fibre reinforced polymer was carried out based on the materials loading rate Θ, and crush distance δ. At decreasing peak crush force, the energy absorption decreases while loading rate and crush distance increases and decreases respectively. The validity of the derived model expressed as; $E = Þe^{\kappa\delta} - ß\ln\theta + N$ was rooted in the core expression $E + ß\ln\theta \approx Þe^{\kappa\delta} + N$ where both side of the expression correspondingly near-equal. Results generated from both experiment and model prediction indicates that energy absorbed decreases with increased loading rate and decreased crush distance. Evaluated results show that the correlations between the energy absorbed and loading rate & crush distance are 0.9780 and 0.9358 & 0.9795 and 0.9810, using model-predicted and experimental results respectively. For every change in the loading rate and crush distance, the overall standard error incurred on predicting the energy absorbed by the fractured composite, relative to experimental results is < 0.05%. The maximum differential between the experimentally determined and model-predicted energy absorption by fractured carbon fibre reinforced polymer is – 0.1046kJ. The energy absorbed by the fractured composite per unit loading rate and crush distance are -1.875×10^{-2} & $-2.26 \times 10^{-2}KJsm^{-1}$ and 19.5567 & 23.5724 $KJsm^{-1}$ as evaluated from experimental and derived model results.

References

Emekwisia, C.C., Ike-Eze, E., Aigbodion, V.S., 2020. Effects of Chemical Reagents on the Properties of Oil Palm Fruit Fiber Composite. Journal of Advancements in Material Engineering, 5(1), pp.11-18. Available at: http://doi.org/10.5281/zenodo.3708978.

Lau, W.S., Yue, T.M., Lee, T.C. and Lee, W.B., 1995. Un-conventional machining of composite materials. Journal of Materials Processing Technology, 48, pp.199-205.

Shanmugam, D.K., Chen, F.L., Siores, E. and Brandt, M., 2002. Comparative study of jetting machining technologies over laser machining technology for cutting composite materials. Composite Structures, 57(1-4), pp.289-296. doi:10.1016/S0263-8223(02)00084-7.

Hernandez-Castaned, J.C., Sezer, H.K. and Li, L., 2011. The effect of moisture content in fibre laser cutting of pine wood. Optics and Lasers in Engineering, 49, pp.1139-1152. doi:10.1016/j.optlaseng.2011.06.003.

Santhanakrishnan, G., Krishnamurthy, R. and Malhotra, S.K., 1988. Machinability characteristics of fibre reinforced plastics composites. Journal of Mechanical Working Technology, 17, pp.195-204. doi:10.1016/0378-3804(88)90029-2.

Williams, J.G., 1989. The fracture mechanics of delamination tests. Journal of Strain Analysis, 24, pp.207-214. doi:10.1243/03093247V244207.

Lasri, L., Nouari, M. and El Mansori, M., 2011. Wear resistance and induced cutting damage of aeronautical FRP components obtained by machining. Wear, 271, pp.2542-2548. doi:10.1016/j.wear.2010.11.056.

Shetty, N., Shahabaz, S.M., Sharma, S.S. and Shetty, S.D., 2017. A review on finite element method for machining of composite materials. Composite Structures, 176, pp.790-802. doi:10.1016/j.compstruct.2017.06.012.

Williams, J.G., 2001. Introduction to linear elastic fracture mechanics. In: D.R. Moore, A. Pavan and J.G. Williams, eds. Fracture Mechanics Testing Methods for Polymers, Adhesives and Composites. ESIS Publication 28. Elsevier, pp.3-10.

Gillespie, J.W., 1991. Damage tolerance of composite structures: the role of interlaminar fracture mechanics. Journal of Offshore Mechanics and Arctic Engineering, 113, pp.247-252. doi:10.1115/1.2919927.

Tay, T.E., 2003. Characterization and analysis of delamination fracture in composites: an overview of developments from 1990 to 2001. Applied Mechanics Reviews, 56, pp.1-31. doi:10.1115/1.1504848.

Davies, P., 2008. Review of standard procedures for delamination resistance testing. In: S. Sridharan, ed. Delamination Behaviour of Composites. Woodhead Publishing, pp.65-86. doi:10.1533/9781845694821.1.65.

Brunner, A.J., Blackman, B.R.K. and Davies, P., 2008. A status report on delamination resistance testing of polymer-matrix composites. Engineering Fracture Mechanics, 75, pp.2779-2794. doi:10.1016/j.engfracmech.2007.03.012.

Brunner, A.J., 2018. Scatter, scope and structures: what fatigue fracture testing of fiber polymer composites is all about. In: Proceedings of the 39th Risø International Symposium on Materials Science, IOP Conference Series: Materials Science and Engineering, 388, pp.1-19. doi:10.1088/1757-899X/388/1/012003.

Donaldson, S.L. and Mall, S., 1989. Delamination growth in graphite/epoxy composites subjected to cyclic mode III loading. Journal of Reinforced Plastics and Composites, 8, pp.91-103. doi:10.1177/073168448900800106.

Martin, R.H., 1991. Evaluation of the split cantilever beam test for mode III delamination testing. In: T.K. O'Brien, ed. Composite Materials: Fatigue and Fracture, vol. 1110, ASTM Special Technical Publication, pp.243-266. doi:10.1520/STP17722S.

Miura, M., Shindo, Y., Narita, F., Watanabe, S. and Suzuki, M., 2009. Mode III fatigue delamination growth of glass fiber reinforced woven polymer laminates at cryogenic temperatures. Cryogenics, 49, pp.407-412. doi:10.1016/j.cryogenics.2009.05.004.

Shindo, Y., Miura, M., Takeda, T., Saito, N. and Narita, F., 2011. Cryogenic delamination growth in woven glass/epoxy composite laminates under mixed-mode I/II fatigue loading. Composites Science and Technology, 71, pp.647-652. doi:10.1016/j.compscitech.2011.01.006.

Miura, M., Shindo, Y., Takeda, T. and Narita, F., 2014. Mixed-mode I/III fatigue delamination growth in woven glass/epoxy composite laminates at cryogenic temperatures. Journal of Composite Materials, 48, pp.1251-1259. doi:10.1177/0021998313484951.

Jaeck, I., Carreras, L., Rernart, J., Turon, A., Martin de la Escalera, F. and Essa, Y., 2018. Experimental methodology for obtaining fatigue crack growth rate curves in mixed-mode I-II by means of variable cyclic displacement tests. International Journal of Fatigue, 110, pp.63-70. doi:10.1016/j.ijfatigue.2018.01.016.

Rubiera, S., Argüelles, A., Viña, J. and Rocandio, C., 2018. Study of the phenomenon of fatigue delamination in a carbon-epoxy composite under mixed mode I/II fracture employing an asymmetric specimen. International Journal of Fatigue, 114, pp.74-80. doi:10.1016/j.ijfatigue.2018.05.015.

Johnson, A.F., Pickett, A.K. and Rozycki, P., 2001. Computational methods for predicting impact damage in composite structures. Composites Science and Technology, 61, pp.2183-2192. doi:10.1016/S0266-3538(01)00120-3.

Greve, L. and Pickett, A.K., 2006. Delamination testing and modelling for composite crash simulation. Composites Science and Technology, 66, pp.816-826. doi:10.1016/j.compscitech.2005.06.015.

Ladeveze, P. and Le Dantec, E., 1992. Damage modelling of the elementary ply for laminated composites. Composites Science and Technology, 43, pp.257-267. doi:10.1016/0266-3538(92)90097-M.

Johnson, A.F., Thomson, R.S., David, M., Joosten, M.W. and Waimer, M., 2015. Design and Testing of Crashworthy Aerospace Composite Components. In: Polymer Composites in the Aerospace Industry. https://doi.org/10.1016/B978-0-080102679-300013-7.

Bisagni, C., Dipietro, G., Fraschini, L. and Terletti, D., 2005. Progressive crushing of fibre-reinforced composite structural components of a formula one racing car. Composite Structures, 68, pp.491-503. doi:10.1016/j.compstruct.2004.04.026.

Federal Aviation Administration, AC20-107B, Advisory circular on composite aircraft structure.

Hachenberg, D., 2002. The role of advanced numerical methods in the design and certification of future composite aircraft structures. In: 5th World Congress on Computational Mechanics, WCCM V, Vienna.

U.S. Department of Energy, 2017. Bandwidth Study on Energy Use and Potential Energy Saving Opportunities in U.S. Carbon Fiber Reinforced Polymer Manufacturing. Office of Energy Efficiency and Renewable Energy (EERE).

Nwoye, C.I., 2008. Data Analytical Memory. C-NIKBRAN.

Cheng, Q., 2005. Load/Displacement and Energy Absorption Performances and Improvements of Structural Members Under Tensile and Compressive Loading Conditions [dissertation]. Windsor: University of Windsor. https://scholar.uwindsor.ca/etd/2630.